VIP Energy Transfer

DOI: 10.1002/anie.201108025

Dynamic Mapping of CN Rotation Following Photoexcitation of ICN^-**

Amanda S. Case, Elisa M. Miller, Joshua P. Martin, Yu-Ju Lu, Leonid Sheps, Anne B. McCoy, and W. Carl Lineberger**

The ICN molecule is a prototype for the study of dynamics at conical intersections;[1] 266 nm photoexcitation to the A continuum[2] produces a bimodal distribution of CN photofragment rotations identified with different I-atom partner fragments [Equations (1) and (2)]:

$$ICN + h\nu \rightarrow I(^2P_{3/2}) + CN(^2\Sigma^+),\ \langle E_{rot}\rangle = 0.41\ eV \quad (1)$$

$$ICN + h\nu \rightarrow I^*(^2P_{1/2}) + CN(^2\Sigma^+),\ \langle E_{rot}\rangle = 0.04\ eV^{[3]} \quad (2)$$

Trajectory calculations that were run on high-level potential energy surfaces[4] established that bending motion, which occurs along with the I–CN bond elongation, maps into torque on the CN as ICN passes through a conical intersection, giving the notably high degree of rotational excitation observed in concurrence with $I(^2P_{3/2})$. Condensed-phase ICN photodissociation studies also observe this significant degree of rotation,[5] and even in the strongly interacting solvent water, the CN fragment is initially born as a free rotor.[6]

In the absence of a conical intersection, the shape of the excited-state potential energy surface still plays a large role in the rotational-state distribution of the photofragments. An isotropic excited-state surface simply converts any original bending motion into rotation of the fragments upon bond cleavage, resulting in a small degree of rotational excitation. However, the presence of anisotropy on the excited-state surface induces torque that initiates additional rotational motion in the fragments and can lead to a much larger degree of rotational excitation. These exit channel dynamics convey the efficiency of translational to rotational energy transfer. The photodissociation of H_2O_2 serves as an instructive example, in which the OH rotational-state distribution reflects both the torsional wavefunction of the electronic ground state and the anisotropy of the excited-state surfaces.[7]

In a confined environment, the relaxation of rotational excitation will influence the subsequent dynamics. Molecular dynamics simulations of ICN photodissociation in solid and liquid Ar were performed on the two excited-state potential energy surfaces ($^3\Pi_{0+}$ and $^1\Pi_1$) that form the conical intersection.[8] These simulations found complete cage recombination in the solid, along with differences in the cage-induced isomerization dynamics; both ICN and INC form on the $^3\Pi_{0+}$ surface, while only ICN is found on the $^1\Pi_1$ surface. In this model, which neglects nonadiabatic transitions, the contrasting anisotropies of the ICN excited-state potential energy surfaces give rise to different rotational-relaxation dynamics. These relaxation dynamics, along with the CN-rotation barriers, are responsible for the dissimilar isomerization yields.

Herein we investigate the excited-state dynamics of $ICN^-(Ar)_n$ for $n = 0$–5 using excitation energies between 2.5 and 4.2 eV. Specifically, we focus on the role of CN fragment rotation in the dynamics of photoexcited ICN^- with and without Ar solvation. Figure 1 sketches potential energy curves adapted from Ref. [9] for the electronic ground state of the ICN^- and INC^- isomers ($^2\Sigma^+$, red) and the first optically accessible excited state of these isomers ($^2\Pi_{1/2}$, blue), along

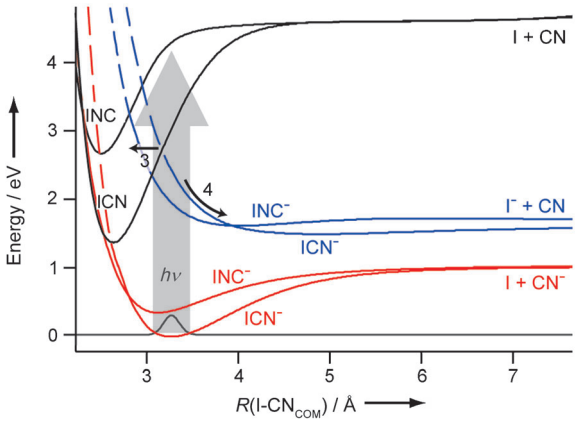

Figure 1. Potential energy curves (based on Ref. [9]) for the ICN^- and INC^- isomers ($^2\Sigma^+$ red, $^2\Pi_{1/2}$ blue) and the ICN and INC isomers ($^1\Sigma^+$ black), as a function of the I–CN center of mass distance. The solid and dashed curves for the anion represent the anion potential being lower and higher than the neutral, respectively. The gray line shows the probability amplitude of the ground-state wavefunction for ICN^-. The arrows illustrate photoexcitation (large gray arrow) and subsequent detachment (3) or dissociation (4).

[*] Dr. A. S. Case,[+] E. M. Miller,[+] J. P. Martin,[+] Y.-J. Lu,[+] Dr. L. Sheps,[$] [+] Prof. W. C. Lineberger[+]
JILA and Department of Chemistry and Biochemistry
University of Colorado, Boulder, CO 80309 (USA)
E-mail: wcl@jila.colorado.edu
Prof. A. B. McCoy[+]
Department of Chemistry, The Ohio State University
Columbus, OH 43210 (USA)
E-mail: mccoy@chemistry.ohio-state.edu
[$] Present address: Sandia National Laboratory
Livermore, CA 94550 (USA)
[+] These authors contributed equally to this work.

[**] We thank the National Science Foundation (WCL Grants CHE-0809391, PHY-1125844 and ABM Grant CHE-0848242), the Air Force Office of Scientific Research (WCL Grant FA9550-09-1-0046), and the Office of Naval Research (ABM Grant N000140910533).
Supporting information for this article is available on the WWW under http://dx.doi.org/10.1002/anie.201108025.

with the electronic ground state of the ICN and INC isomers ($^1\Sigma^+$, black). Figure 1 also depicts photoexcitation of ground-state ICN^-, which undergoes either electron detachment [Equation (3)] or dissociation [Equation (4)] through the following channels:

$$ICN^-(Ar)_n + h\nu \rightarrow ICN(Ar)_n + e^- \quad (3)$$

$$\rightarrow ICN^-(Ar)_{m<n} + (n-m)Ar \quad (4a)$$

$$\rightarrow I^-(Ar)_{m\leq n} + CN + (n-m)Ar \quad (4b)$$

$$\rightarrow CN^- + I + n\,Ar \quad (4c)$$

We investigate all four product pathways using a photoelectron velocity-map imaging spectrometer to collect electron signals[10] or a secondary mass analyzer (10 μs flight) for detection of ionic photoproducts.[10]

Along with direct detachment, photodetachment produces neutral ICN together with low-kinetic-energy (KE) electrons that have a KE independent of the photon energy. Beyond the expected photodissociation products, the addition of a single Ar atom (which is only bound by about 50 meV[11]) results in the formation of recombined ICN^-. The common theme of these experimental findings is the large amount of internal energy that must be deposited into the neutral or anion product. For the photon energies used in these experiments, most of the excess energy is in the I–C bond. Energy transfer between the low-frequency I–C stretch and the high-frequency C–N stretch will be inefficient. In contrast, quantum dynamics calculations indicate quick and efficient energy transfer into CN rotation following photoexcitation. Thus, it is likely that CN rotation plays a vital role in storing considerable amounts of internal energy.

The extraordinary energy-storage ability of ICN can be seen in electron photodetachment from ICN^-. Direct detachment produces a standard photoelectron spectrum that is readily characterized in terms of neutral ICN electronic states.[11] However, for photon energies between 2.5 and 4.2 eV, photodetachment produces additional discrete low-KE electrons (5–10% of total).[10] These photon energies are insufficient for dissociative photodetachment and, as such, the ICN product (EA(ICN) = 1.35 eV[11]) must contain 1.15 to 2.85 eV of internal energy. This high degree of internal energy permits access to both the ICN and INC isomers. As Figure 2 shows, the indirect detachment signal in the spectrum has a shape that is independent of the photon energy. Additionally, the spectrum remains unchanged in the photodetachment of $ICN^-(Ar)$. Electron ejection by an indirect process must occur with a time delay following photoabsorption. The relative cross-section (see Figure 2) for this process is consistent with two peaks that are optically allowed ICN^- doorway states into a dense ICN^- bath, from which quasi-thermal electron emission occurs. CN rotation, hindered or free, will be essential toward obtaining a sufficient density of states to allow the anion to act as a heat bath.

The 2.5 eV excitation of ICN^- yields predominantly I^- + CN products. For $ICN^-(Ar)_n$ (n = 1–5), I^--based products remain the dominant channel in the photodissociation but with an unexpectedly high degree of fragment-ion solvation.[10] For example, $I^-(Ar)_2$ is the most abundant product of $ICN^-(Ar)_2$ photodissociation. This dominance of solvated products requires that excess energy is transferred into internal excitation of the fragments and not into solvent evaporation. These results are in stark contrast to previous studies on dihalides,[12] where the solvent loss from caged products follows the evaporative ensemble model, dissipating excess energy through evaporation of the neutral solvent.[13]

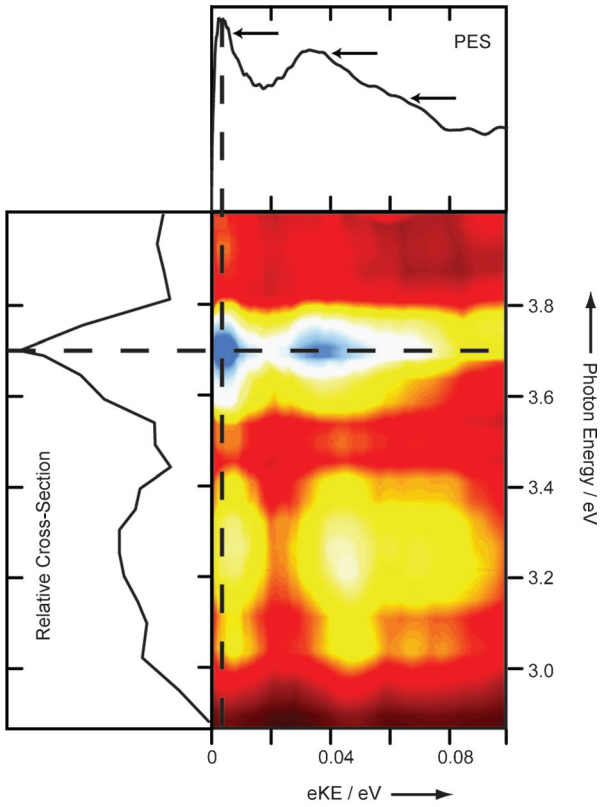

Figure 2. Partial photoelectron spectrum (PES) of ICN^- showing the intensity for the most prominent region of low-KE electron signal as a function of electron kinetic energy (eKE) and photon energy. Top trace: PES at a photon energy of 3.7 eV showing the low-KE electron features (indicated with arrows). Left-hand trace: relative cross-section for producing the feature near 0 eV, over the photoexcitation range shown (2.9 to 4.0 eV).

Our photodissociation studies also find a roughly 6% recombination yield for $ICN^-(Ar)_{1-5}$. Cage recombination for a single Ar solvent is particularly surprising, especially for such a weakly bound solvent. Moreover, the independence of the caging fraction on n shows that a single, labile Ar is crucial for recombination. The Ar–ICN^- potential is relatively isotropic, allowing Ar to sample large regions of configuration space about the chromophore. This leads to an occasional collision between Ar and the departing CN fragment. Recombination to stable ICN^- products cannot occur on a dissociative state. Yet, ICN^- signal persists for more than 10 μs after photoexcitation, indicating that stable parent anions indeed re-form. The weak binding energy of the Ar solvent (ca. 50 meV) is insufficient to bridge the large energy separation between the $^2\Pi_{1/2}$ state and the bound ground state (800 meV). Meanwhile, ab initio calculations do find a shallow (ca. 270 meV) potential well on the $^2\Pi_{1/2}$ surface of ICN^-.[9]

The only way that recombined anions can be trapped on the excited $^2\Pi_{1/2}$ surface is for a large fraction of the available energy to be tied up in rotation of the CN moiety, forming a complex between I^- and the trapped free rotor CN. This [I^-—CN] complex formation allows sufficient time for radiative transfer back to the ground state, where a stable ICN^- can form.

Additional evidence for the importance of the free internal rotation of CN in [I^-—CN] comes from quantum dynamics calculations of the photodissociation of bare ICN^- on the $^2\Pi_{1/2}$ potential energy surface.[10] Promoting the rovibronic ground-state wavefunction ($J_{tot}=0$) of the anion onto the $^2\Pi_{1/2}$ surface results in an increase in the I–CN distance (R coordinate) owing to the dissociative nature of the excited state. The calculations also show that the wavefunction spreads quickly along the CN rotational degree of freedom (θ coordinate). The anisotropy of the $^2\Pi_{1/2}$ potential efficiently couples R and θ, allowing the excited ICN^- to explore both internal coordinates as it dissociates. As illustrated in Figure 3, at $t=0$ the wavefunction only has amplitude for values of θ less than 50°; however, by 180 fs the wavefunction has amplitude over all I–CN bend angles, effectively making CN a free rotor. After 360 fs, the I–CN separation has increased to about 12 Å, and essentially all CN orientations are equally probable. The calculations also show that about 20% of the available energy is partitioned into CN rotation; furthermore, this fraction increases with initial bend excitation. Additional calculations, artificially altering the time scale of the CN rotation with respect to the ICN^- dissociation, illustrate that the longer CN samples the anisotropic portions of the potential energy surface, the more energy will go into rotation.

The calculations of bare ICN^- dynamics point to a mechanism for the one-atom cage effect that we observe in ICN^-(Ar). In a small portion of the excited population, collision of the CN fragment with Ar reduces the excess energy remaining with the I^- and CN components. Additionally, the relatively slow dissociation of ICN^- allows ample time to sample the anisotropic portions of the excited-state potential energy surface, thus populating a reasonable degree of rotational excitation in the CN fragment. Taken together, these two processes tie up a considerable amount of energy, allowing the [I^-—CN] complex a substantial excited-state lifetime and, thus, a non-negligible radiative transition probability. This mechanism gains support from photodissociation studies of neutral ICN in a cryogenic matrix, detecting emission following cage-induced trapping on a weakly bound excited-state surface.[14]

Despite the lack of a conical intersection, the dynamics of photoexcited ICN^- result in a highly rotationally excited CN fragment. The ability of ICN^- to sequester substantial amounts of energy in CN rotation enables both single-solvent caging and the production of highly solvated photodissociation products. Additionally, this CN rotor allows the photoexcited anion to serve as its own heat bath, thus enabling quasi-thermionic electron emission. In all cases, CN rotation (hindered or free) is a crucial part of the intramolecular energy flow pathways and a major sink for internal energy.

Received: November 15, 2011
Published online: February 1, 2012

Keywords: intramolecular energy transfer · molecular dynamics · one-atom caging · photochemistry

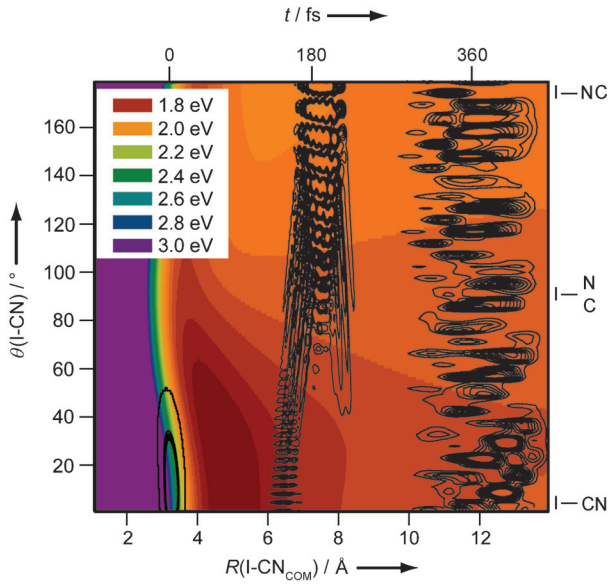

Figure 3. Quantum dynamics calculation results for $t=0$, 180, and 360 fs following promotion of the ICN^- $^2\Sigma^+$ rovibronic ground-state wavefunction ($J_{tot}=0$) to the $^2\Pi_{1/2}$ surface. Upper axis: propagation times approximately corresponding to the increasing I–CN distance. The probability amplitude (black contours) is shown on the $^2\Pi_{1/2}$ potential energy surface (color) as a function of the Jacobi coordinates R and θ.

[1] For example, see the reviews and references in: a) J. F. Black, J. R. Waldeck, R. N. Zare, *J. Chem. Phys.* **1990**, *92*, 3519; b) G. Hancock, G. Richmond, G. A. D. Ritchie, S. Taylor, M. L. Costen, G. E. Hall, *Mol. Phys.* **2010**, *108*, 1083.
[2] W. P. Hess, S. R. Leone, *J. Chem. Phys.* **1987**, *86*, 3773.
[3] I. Nadler, D. Mahgerefteh, H. Reisler, C. Wittig, *J. Chem. Phys.* **1985**, *82*, 3885.
[4] a) Y. Amatatsu, S. Yabushita, K. Morokuma, *J. Chem. Phys.* **1994**, *100*, 4894; b) J. Qian, D. J. Tannor, Y. Amatatsu, K. Morokuma, *J. Chem. Phys.* **1994**, *101*, 9597.
[5] a) A. C. Moskun, S. E. Bradforth, *J. Chem. Phys.* **2003**, *119*, 4500; b) A. C. Moskun, A. E. Jailaubekov, S. E. Bradforth, G. Tao, R. M. Stratt, *Science* **2006**, *311*, 1907.
[6] C. A. Rivera, N. Winter, R. V. Harper, I. Benjamin, S. E. Bradforth, *Phys. Chem. Chem. Phys.* **2011**, *13*, 8269.
[7] R. Schinke, V. Staemmler, *Chem. Phys. Lett.* **1988**, *145*, 486.
[8] A. I. Krylov, R. B. Gerber, *J. Chem. Phys.* **1994**, *100*, 4242.
[9] A. B. McCoy, *Int. J. Quantum Chem.* **2012**, DOI: 10.1002/qua.24011.
[10] See the Supporting Information for additional information.
[11] E. M. Miller, L. Sheps, Y.-J. Lu, A. S. Case, A. B. McCoy, W. C. Lineberger, *J. Chem. Phys.* **2012**, DOI: 10.1063/1.3679170.
[12] See, for example: V. Vorsa, S. Nandi, P. J. Campagnola, M. Larsson, W. C. Lineberger, *J. Chem. Phys.* **1997**, *106*, 1402.
[13] C. E. Klots, *Z. Phys. D* **1987**, *5*, 83.
[14] J. Helbing, M. Chergui, S. Fernandez-Alberti, J. Echave, N. Halberstadt, J. A. Beswick, *Phys. Chem. Chem. Phys.* **2000**, *2*, 4131.

